Available online at www.sciencedirect.com
SCIENCE DIRECT®
Journal of Catalysis 224 (2004) 384–396
JOURNAL OF CATALYSIS
www.elsevier.com/locate/jcat

Investigation on the catalysis of CO_x-free hydrogen generation from ammonia

Shuang-Feng Yin,[a,b] Qin-Hui Zhang,[a] Bo-Qing Xu,[a,*] Wen-Xia Zhu,[b,c] Ching-Fai Ng,[b] and Chak-Tong Au [b,*]

[a] *Innovative Catalysis Program, Key Lab of Organic Optoelectronics & Molecular Engineering, Department of Chemistry, Tsinghua University, Beijing 100084, China*

[b] *Department of Chemistry, Center for Surface Analysis and Research, Hong Kong Baptist University, Kowloon Tong, Hong Kong, China*

[c] *Department of Chemistry, Xiamen University, Xiamen 361005, China*

Received 27 November 2003; revised 23 February 2004; accepted 3 March 2004

Available online 20 April 2004

Abstract

The effects of active component (Ru, Rh, Pt, Pd, Ni, Fe) and support (CNTs, AC, Al_2O_3, MgO, ZrO_2, TiO_2) on the catalysis of ammonia decomposition were studied for the generation of CO_x-free hydrogen. It was shown that the Ru catalyst using CNTs as support exhibits the highest conversion of NH_3. The performance can be further improved by modifying CNTs with KOH. According to the results of XRD, TEM, and chemisorption (CO and H_2 as adsorbates) investigations, Ru dispersion is the highest on CNTs. In the range of 2–5 nm, the particle size of Ru on CNTs is the smallest among the supported Ru catalysts; the Ru particles on the metal oxides are in the 3–16 nm range. It seems that larger Ru particles are more active for NH_3 decomposition in terms of TOF. Further investigation on the relationship between support basicity and catalytic activity disclosed that a support material of strong basicity is essential for high catalytic performance. In the N_2-TPD studies of supported Ru catalysts, desorption was promoted over catalysts of strong basicity, suggesting that N_2 desorption is the rate-determining step in ammonia decomposition. These results implied that it is possible to develop a highly efficient Ru catalyst for NH_3 decomposition by using electron-conductive materials of strong basicity as support.

Keywords: Carbon nanotubes; Ruthenium; Ammonia decomposition; Hydrogen generation; Basicity; Nanocatalysis

1. Introduction

The concern for environmental protection has risen dramatically over the past two decades. In order to eliminate pollution that arises from automobile exhaust and small-scale power units, on-site hydrogen generation for proton-exchange membrane fuel cells (PEMFC) is a topic of current interest [1]. The option of producing hydrogen directly from carbonaceous substances (e.g., methanol, methane) has its limitation because the by-product CO_x ($x = 1, 2$), even at extremely low concentrations, degrades the cell performance [2–6]. The use of ammonia (NH_3) as a hydrogen provider appears to be attractive because it produces no CO_x, and the unconverted NH_3 can be reduced to less than 200 ppb level by means of a suitable adsorber [1]. It has been pointed out that it is more economical to generate H_2 via NH_3 decomposition than via methanol reforming [7,8]. Traditionally, research conducted on the catalytic decomposition of NH_3 is mainly devoted to the understanding of the catalysis of NH_3 synthesis and/or NH_3 abatement [9–17]. The reaction was usually conducted under diluted conditions for mechanistic studies. Recently, a number of papers have been published and patents filed for H_2 generation from ammonia [18–23]. However, a reaction temperature higher than 873 K was required for satisfactory activity over these catalysts. Based on thermodynamic data at 298 K [24], the following equation can be adopted for the calculation of equilibrium conversion in NH_3 decomposition at normal pressure (1.01325×10^5 Pa):

$$\left[40100 - (25.46T \ln T) + \left(0.00917T^2\right) - (103000/T) + 64.81T\right] = -RT \ln\left[1.3X^2/\left(1 - X^2\right)\right],$$

* Corresponding authors. Fax: 86 10 62792122.
E-mail addresses: bqxu@mail.tsinghua.edu.cn (B.-Q. Xu), pctau@hkbu.edu.hk (C.-T. Au).

0021-9517/$ – see front matter
doi:10.1016/j.jcat.2004.03.008

Table 1
Equilibrium conversion of NH_3 at different temperatures and 1 atm[a]

Temperature (K)	523	573	623	643	673	693	723	743	773
Conversion (%)	89.21	95.69	98.12	98.61	99.11	99.31	99.53	99.63	99.74

[a] $NH_3(g) \rightleftharpoons \frac{1}{2}N_2\ (g) + \frac{3}{2}H_2(g)$, $\Delta rH^0m(NH_3(g), 298.15\ K) = -46.19$ kJ/mol, $\Delta rG^0m(NH_3(g), 298.15\ K) = -16.63$ kJ/mol, $\Delta C_p = 25.46 - 0.01833T + 205000T^{-2}$.

where T and X are reaction temperature (K) and equilibrium NH_3 conversion (%), respectively. Listed in Table 1 are the related data; one can see that at 673 K, the equilibrium conversion is 99.1%. Above 673 K, the conversion becomes less dependent on temperature. In the viewpoint of thermodynamics, it is possible to develop active catalysts for complete NH_3 decomposition at around 673 K.

In a recent communication, we reported that the use of multiwall carbon nanotubes (CNTs) as support for Ru resulted in a highly active Ru/CNTs catalyst for NH_3 decomposition [25]. In order to understand the roles of the support and to investigate further the catalysis for complete NH_3 decomposition, we conducted a systematic investigation on the effects of active metals (Ru, Rh, Pt, Pd, Ni, Fe) on the reaction with CNTs being the support material. Then CNTs was compared with a number of other materials (Al_2O_3, activated carbon (AC), MgO, TiO_2, ZrO_2, and ZrO_2-BD) as a support for Ru catalyst. To understand the effect of surface basicity on the catalysis, we modified neutral CNTs and acidic ZrO_2-BD with KOH for comparison purposes.

2. Methods

2.1. Preparation and pretreatment of catalyst support

The employed CNTs (i.d. 3–10 nm, OD 6–20 nm, ratio of length to diameter 100–1000, specific surface area 224 m^2/g) were prepared by the CVD method using Fe/Al_2O_3 as catalyst [26]. The surface area of the commercially available activated carbon (AC) was 1220 m^2/g. The Al_2O_3, MgO, TiO_2, and ZrO_2 (A.R.) materials were purchased from the Beijing Chemical Plant, China. A ZrO_2-BD support of high surface area was also adopted; this material was prepared by reflux digestion in a glass vessel of $ZrO(OH)_2$ in an aqueous NH_4OH solution at pH 11.5 according to the procedures described by Yin and Xu [27]. The calcination temperature of this ZrO_2-BD support was 873 K. The raw CNTs were purified in 5 M aqueous HNO_3 solution for 2 h by means of refluxing, followed by calcination at 973 K in H_2 flow for 2 h. For support modification, potassium was impregnated onto ZrO_2-BD and the purified CNTs from a KOH/ethanol solution, followed by calcination at 773 K for 5 h in Ar flow. The metal oxide supports were calcined at 873 K for 5 h prior to the loading of active metal component. The specific surface areas of the support materials are listed in Table 4.

2.2. Catalyst preparation

All the catalysts were prepared by wetness incipient impregnation with acetone as solvent, followed by drying at 328 K for 5 h and calcination at 823 K for 2 h in Ar flow. The precursors of the active metals were $H_2PtCl_6 \cdot H_2O$, $PdCl_2$, $RuCl_3 \cdot xH_2O$, $RhCl_3 \cdot xH_2O$, $Ni(NO_3)_2 \cdot 6H_2O$, and $Fe(NO_3)_3 \cdot 9H_2O$ (analytic grade), respectively, and were purchased from Aldrich Chemical Company, Ltd. The desired loadings of the active components in the catalysts were 4.95×10^{-4} mol per g catalyst. The K/Ru atomic ratios in the RuK/CNTs and RuK/ZrO_2-BD catalysts were 1.

2.3. Catalytic testing

Catalytic testing was carried out on a continuous flow quartz reactor (catalyst: 100 mg, 60–80 mesh or 180–200 mesh) under pure ammonia atmosphere [NH_3 purity, 99.99%; flow rate, 50 ml/min; $GHSV_{NH_3} = 30{,}000$ ml/(h g_{cat}); another flow rate, 250 ml/min; $GHSV_{NH_3} = 150{,}000$ ml/(h g_{cat})]. Prior to the reaction, the metal (Ru, Rh, Pt, Pd) catalyst was reduced in situ in a 25% H_2/Ar flow at 773 K for 2 h and then purged with pure argon. The reaction temperature was in the range of 623–873 K. The reduction temperature for Ni and Fe catalysts was 973 K. Product analysis was performed on an on-line GC-8A gas chromatograph (Shimadzu) equipped with a thermal conductivity detector and a Poropak Q column, using Ar as carrier gas. We found that ammonia conversion observed in a blank reactor or over the supports was less than 0.2% at 773 K.

2.4. Characterization

The actual loadings of the active components and the contents of residual chlorine in the prepared catalysts were determined on a sequence XRF-1700 X-ray fluorescent spectrometer (Shimadzu), at a setting of 40 kV and 95 mV. The BET surface areas of the supports and catalysts were measured on a Micromeritics 2010C instrument; before each measurement, the sample was heated to 573 K and kept at this temperature for 5 h. The same instrument was used for the measurement of CO- and H_2-chemisorption uptakes at 313 K. Prior to each measurement, the sample was first reduced in H_2 flow at 773 K for 2 h, followed by 1 h evacuation.

Powder X-ray diffraction experiment was conducted on a Rigaku Automatic Diffractometer (Rigaku D-MAX) with

monochromatized Cu-K_α radiation ($\lambda = 0.15406$ nm) at a setting of 40 kV and 80 mA. The patterns recorded were referred to the powder diffraction files-1998 ICCD PDF Database for identification. TEM was used to investigate the morphologies and particle sizes of the catalysts. Images were taken on a JEM-2010F transmission electron microscope operating at 200 kV.

Temperature-programmed reduction (TPR) was operated according to the following steps. Prior to each measurement, the sample (0.1 g) was heated from room temperature (RT) to 623 K with a heating rate of 10 K/min under Ar flow (40 ml/min) and kept at this temperature for 30 min for the removal of adsorbed impurities (e.g., H_2O). After the sample was cooled to RT, the gas flow was switched to 5% H_2/Ar (40 ml/min). Finally, TPR profiles were obtained with a temperature ramp of 10 K/min using a thermal conductivity detector. Before entering the detector, the gases from the TPR reactor were passed through a glass tube filled up with 4A molecular sieve and cooled to ca. 177 K to ensure complete elimination of any water in the gases. Calibration of the TPR peak area for absolute H_2 consumption was made by reducing a series of standard CuO samples. The reducibility of the loaded metal component was estimated based on the amount of H_2 consumption.

The N_2-TPD experiment was carried out using the mass analyzer of a HP4890 GC-MS instrument as the detector. Before the measurement, the catalyst was heated at 623 K and reduced with 20% H_2–Ar at 773 K for 1 h. Then the gas flow was switched to pure He for purging at 773 K for 30 min, and the gas flow was switched to N_2 and the sample was cooled slowly to RT and kept at RT for 20 min. Then, the gas flow was switched to pure He (40 ml/min). A stable baseline was established after a flow of He at RT for 30 min, and the catalyst was heated (10 K/min) and the N_2-TPD curve was recorded. The desorbed amount was calibrated against a standard pulse of N_2 via a sampling tube of 10 µl.

The procedure for the NH_3- or CO_2-TPD experiment of support was similar to that described previously [28]. The carrier gas was pure He, and the gases for adsorption were 1% NH_3/He and high-purity CO_2, respectively. The detector was MSC-200 quadrupole mass spectrometer from Balzer Company, Ltd.

3. Results

3.1. Investigation on active component

In tests that lasted tens of hours, we observed stable performance for ammonia decomposition over all the catalysts. Shown in Fig. 1 and Table 2 are the NH_3 conversion and H_2 formation rate over the different CNT-supported catalysts recorded at a time on stream (TOS) of 3 h, respectively. The particle size of catalysts was 60–80 mesh, and the decomposition reaction was conducted at $GHSV_{NH_3} = 30{,}000$ ml/(h g_{cat}). One can see that at 623 K, the NH_3 conversion over Ru/CNTs is 6.31%, 8–40 times larger than those observed over the supported Rh, Ni, Pt, Pd, and Fe catalysts at equal temperature; and the corresponding H_2 formation rate is 2.11 mmol/(min g_{cat}). Since NH_3 decomposition is an endothermic process ($\Delta H = 11$ kcal/mol; 45.98 kJ/mol), an increase in reaction temperature would result in an enhancement in NH_3 conversion [18]. In the range of 623–773 K, elevation of reaction temperature leads to a drastic increase of the absolute difference in NH_3 conversion over the catalysts. At 773 K, the conversion (84.65%) over the Ru catalyst approximates equilibrium value (99.74%). The H_2 formation rate over Ru/CNTs is ca. 28.35 mmol/(min g_{cat}) at 773 K. We found that under similar reaction conditions, Ru/CNTs (e.g., 17.14% NH_3 conversion at 673 K) is superior to 10% Ru/SiO_2 (14.3% NH_3 conversion at 673 K), the most active catalyst recorded in Goodman and co-workers' work [18]. Since the space velocities of NH_3 adopted in evaluation of the catalysts are identical, a change in NH_3 conversion reflects the variation of H_2 formation rate over the catalysts at different temperatures. Therefore, Ru can be regarded as the most suitable for NH_3 decomposition. Goodman and co-workers [18] reported that over the SiO_2-supported metal

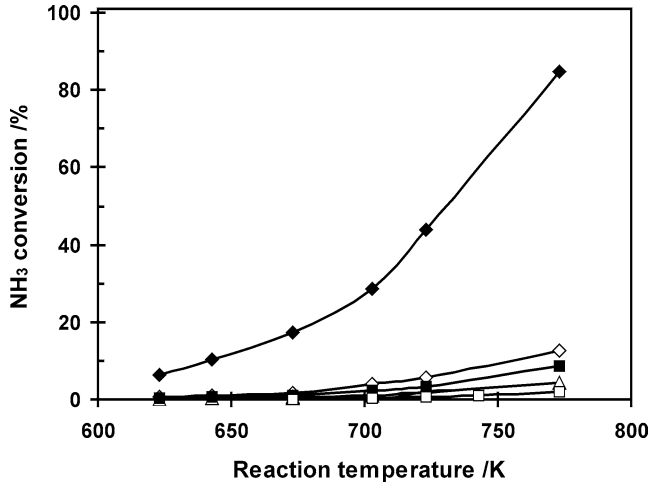

Fig. 1. NH_3 conversion over CNT-supported metal catalysts (◆, Ru; ◇, Rh; ■, Ni; △, Pd; □, Fe; ▲, Pt), $GHSV_{NH_3} = 30{,}000$ ml/(h g_{cat}).

Table 2
H_2 formation (mmol/(min g_{cat})) over the CNT-supported metal catalysts[a]

Reaction temperature (K)	Ru	Rh	Pt	Pd	Ni	Fe
623	2.11	0.2	0.05	0.03	0.10	–
643	3.42	0.34	0.10	0.07	0.17	0.02
673	5.73	0.6	0.21	0.15	0.33	–
703	9.51	1.38	0.37	0.3	0.74	0.07
723	14.64	1.94	0.61	0.57	1.11	0.17
743	–	–	–	–	–	0.34
773	28.35	4.19	1.41	1.43	2.90	0.65

[a] The molar loadings of the active metal in the catalysts are ca. 4.75×10^{-4} mol/g_{cat}, which corresponds to a 5% weight loading for Ru; $GHSV_{NH_3} = 30{,}000$ ml/(h g_{cat}); the data are averaged within initial TOS of 3 h.

catalysts for NH_3 decomposition, Ru was more active than Ni and Ir. It has been suggested that Ru is an attractive catalyst for NH_3 synthesis because Ru/C, a commercialized product, is much more active than the conventional Fe-based catalyst [29].

3.2. Investigation on catalyst support

In the evaluation of catalytic efficiency of Ru catalysts, we adopted a high reaction space velocity (flow rate, 250 ml/min; $GHSV_{NH_3} = 150{,}000$ ml/(h g_{cat})) and very small catalyst particle size (180–200 mesh). Since the effect of mass transfer would become a genuine concern at high reaction rates, all the tests of the present study were carried out at conditions of $\Phi < 1$, where there would be no mass-transfer limitations during the reactions according to the Weisz criterion [30], $\Phi = (dN/dt)(1/C_0)(R^2/D_{eff})$, where dN/dt is the reaction rate (mol/(cm^3 s)), C_0 reactant concentration (mol/cm^3), R particle radius (cm), and D_{eff} effective diffusivity (cm^2/s). It should be noted that both CNTs and AC (unlike the metal oxide supports) are relatively fragile, leading to a gradual size reduction of the catalysts. Therefore, the calculated Φ value for the CNT- or AC-based catalysts is higher than the theoretical one.

Depicted in Fig. 2 are the NH_3 conversions over the supported Ru catalysts at $GHSV_{NH_3} = 150{,}000$ ml/(h g_{cat}), and listed in Table 3 are the corresponding H_2 formation rates. It is obvious that within the temperature range of 623–773 K, although the data of Table 3 were obtained at a NH_3 space velocity 4 times that adopted for the collection of the data in Table 2, no significant difference in H_2 formation rate was observed at similar reaction temperatures for the same Ru/CNTs catalyst, thus providing direct evidence for the absence of mass-transfer limitations in the present study. Moreover, the order of NH_3 conversion can be ranked as Ru/CNTs > Ru/MgO > Ru/TiO_2 ≅ Ru/Al_2O_3 ≅ Ru/ZrO_2 > Ru/AC > Ru/ZrO_2-BD, signifying that Ru/CNTs are indeed the most active. In other words, among the support materials studied, CNTs are the most suitable support for Ru catalyst.

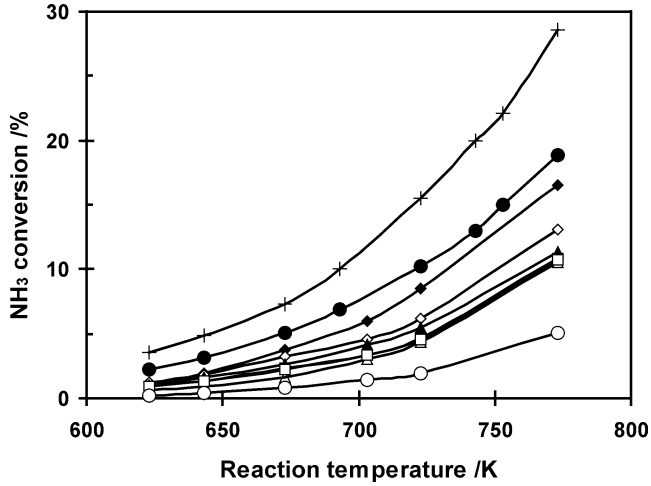

Fig. 2. NH_3 conversion over 5 wt% Ru catalysts supported on various materials (+, K/CNTs; ◆, CNTs; ◇, MgO; ▲, TiO_2; △, AC; □, ZrO_2; ■, Al_2O_3; ○, ZrO_2-BD; ●, K/ZrO_2-BD), $GHSV_{NH_3} = 150{,}000$ ml/(h g_{cat}).

In ammonia synthesis, alkali or alkaline earth ions are used as efficient promoters for supported Ru or Fe catalysts; they are also effective adjuvants for preventing Ru or Fe from sintering [31–33]. Here, we modified CNTs and ZrO_2-BD with KOH; then RuK/CNTs and RuK/ZrO_2-BD catalysts were obtained by impregnating the modified supports with $RuCl_3$ dissolved in acetone, respectively. The catalytic results at $GHSV_{NH_3} = 150{,}000$ ml/(h g_{cat}) are shown in Fig. 2 and Table 3. At 623 K, NH_3 conversion and H_2 formation rate over RuK/CNTs are 3.54% and 5.93 mmol/(min g_{cat}), respectively, much higher than those over Ru/CNTs. However, compared to a KOH-modified Ru/CNTs catalyst [15], it is lower in activity. At 773 K, NH_3 conversion over RuK/CNTs is 28.60%, and the corresponding H_2 formation rate is 47.88 mmol/(min g_{cat}). When the reaction was carried out at $GHSV_{NH_3} = 30{,}000$ ml/(h g_{cat}) and 773 K, there was no detectable ammonia in the effluent, showing that NH_3 conversion was close to the equilibrium level (99.74%). Similar enhancement in activity was observed for Ru catalyst supported on a KOH-modified ZrO_2-BD sample. In ammonia synthesis, Aika and

Table 3
Effect of support on H_2 formation (mmol/(min g_{cat})) over supported Ru catalysts at different reaction temperatures[a]

Reaction temperature (K)	CNTs	MgO	TiO_2	AC	Al_2O_3	ZrO_2	ZrO_2-BD	KCNTs	KZrO_2-BD
623	2.01	1.98	1.67	0.97	1.51	1.42	0.40	5.93	3.65
643	3.30	3.11	2.68	1.51	2.24	2.09	0.67	8.12	5.29
673	6.23	5.42	4.35	2.68	3.85	3.68	1.32	12.22	8.54
693	–	–	–	–	–	–	–	16.81	11.55
703	10.08	7.67	6.90	5.02	5.59	5.52	2.41	–	–
723	14.28	10.35	9.11	7.37	7.87	7.20	3.23	25.95	17.07
743	–	–	–	–	–	–	–	33.48	21.76
753	–	–	–	–	–	–	–	37.00	25.11
773	27.74	22.43	18.93	17.58	18.08	16.24	8.54	47.88	31.64

[a] The molar loadings of Ru in the catalysts are ca. 4.75×10^{-4} mol/g_{cat}, and the ratio of K/Ru is 1 in the RuK/CNTs and RuK/ZrO_2-BD catalysts; $GHSV_{NH_3} = 150{,}000$ ml/(h g_{cat}); the data are averaged within initial TOS of 3 h.

co-workers [32], observed no marked difference in activities over RuK/MgO and Ru/MgO. We also found that the modification of MgO with KOH does not result in a remarkable increase in activity (not shown here). Thus, the modification effect of the alkali metal ions is dependent on the nature of support materials and the reaction system.

4. Characterization

The decomposition steps of NH_3 are sensitive to the structure and texture of support and metal catalyst. In order to investigate the essential factors that affect catalytic performance, we employed XRF, BET, XRD, TEM, H_2-TPR, CO (H_2)-chemisorption, and N_2-TPD techniques to characterize the catalysts.

4.1. Elemental analysis

The designed loadings of active component were 4.95×10^{-4} mol per gram of catalyst, which corresponds to a weight percentage of 5% for the Ru catalysts. According to the color of the precursor metal salts, one can have a rough estimation on the successfulness of loading the metals on the supports. If there was no color implanted on the inner wall of the glass container used for impregnation, the actual loading could be considered as close to the intended value. After impregnation and drying processes, we observed no color implantation on the wall of the container, and deduced that the actual content of the active component should be close to 4.95×10^{-4} mol/g_{cat}. The results of XRF measurement (Table 4) revealed that the actual contents of active metal in the prepared samples (except the modified ones) were in the range of 4.6–4.9 $\times 10^{-4}$ mol/g_{cat}, suggesting that the metals were loaded nearly completely on the supports.

The XRF results (in Table 4) also showed that the molar ratios of Cl/metal in the present catalysts of unmodified support were in the range of 0.003–0.061. For the Fe/CNTs and Ni/CNTs catalysts, the Cl/metal ratios are very small; they are 0.003 and 0.007, respectively. Therefore, we deduce that the Cl^{-1} ions are originated from the precursor of the corresponding metal component, and the H reduction at 773 K could almost lead to the complete removal of Cl^{-1}. The reduced RuK/CNTs and RuK/ZrO_2-BD catalysts, however, show a molar Cl/Ru ratio of 0.284 and 0.258, respectively. The high content of Cl in these two catalysts is a result of KOH interaction with $RuCl_3$, and the KCl generated is a stable compound under hydrogen [40].

4.2. BET surface area

From Table 4, one can see that among the supports, there are significant discrepancies in surface area. For example, the surface area of activated carbon is 1220 m^2/g, while that of CNTs is 224 m^2/g. The metal oxide supports except ZrO_2-BD (289 m^2/g) exhibit surface areas in the range of 6–189 m^2/g, much lower than the carbon materials. The loading of metals on these support materials led to a slight decrease in specific surface area.

4.3. NH_3 and CO_2-TPD

Fig. 3 depicts the NH_3-TPD profiles of the supports. No signals of NH_3 desorption were observed over AC, CNTs, KOH-modified CNTs, and KOH-modified ZrO_2-BD, signifying that there were no acidic sites on these materials. Broad signals ranging from RT to 723 K were observed over TiO_2, ZrO_2, Al_2O_3, and ZrO_2-BD. It is obvious that ZrO_2-BD is the strongest in acidity and the largest in number of acidic sites.

Table 4
Properties of catalysts employed in ammonia decomposition

Catalyst	Surface area (m^2/g)		Cl/M[b]	Loading	Ru particle sizes by TEM (nm)		Dispersion[c]
	Support	Catalyst		(μmol/g_{cat})	Size range	Average size[a]	(%)
Ru/CNTs	224	168	0.058	464	2-5	3.9	25.6
Rh/CNTs	224	171	0.044	469	–	–	–
Pt/CNTs	224	172	0.035	481	–	–	–
Pd/CNTs	224	162	0.061	476	–	–	–
Fe/CNTs	224	174	0.003	482	–	–	–
Ni/CNTs	224	170	0.007	486	–	–	–
Ru/AC	1220	1130	0.056	469	2–5	4.1	24.4
Ru/MgO	24	13	0.021	477	2–15	9.1	11.0
Ru/Al_2O_3	159	108	0.024	480	3–16	8.7	11.5
Ru/TiO_2	6	3	0.022	469	–	–	–
Ru/ZrO_2	30	19	0.022	475	–	–	–
Ru/ZrO_2-BD	289	223	0.012	481	4–16	9.4	10.6
RuK/CNTs	189	147	0.284	447	2–5	3.7	27.0
RuK/ZrO_2-BD	264	227	0.258	438	–	–	–

[a] Estimated by the equation: $d_n = \sum n_i d_i / \sum n_i$ from Ref. [39] based on TEM data.
[b] M, active metal component; Cl/M, molar ratio of the residual chlorine ion to the active metal, measured by XRF.
[c] The dispersion is obtained according to the average size of Ru.

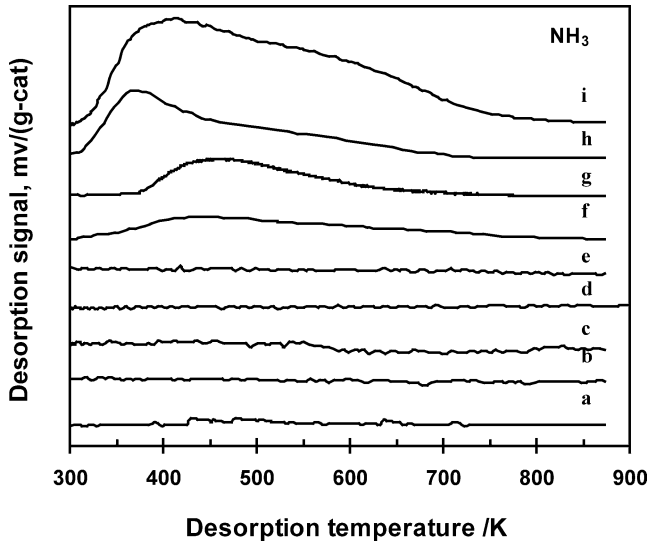

Fig. 3. NH_3-TPD curves of supports (a, AC; b, CNTs; c, K/CNTs; d, K/ZrO_2-BD; e, MgO; f, TiO_2; g, ZrO_2; h, Al_2O_3; i, ZrO_2-BD).

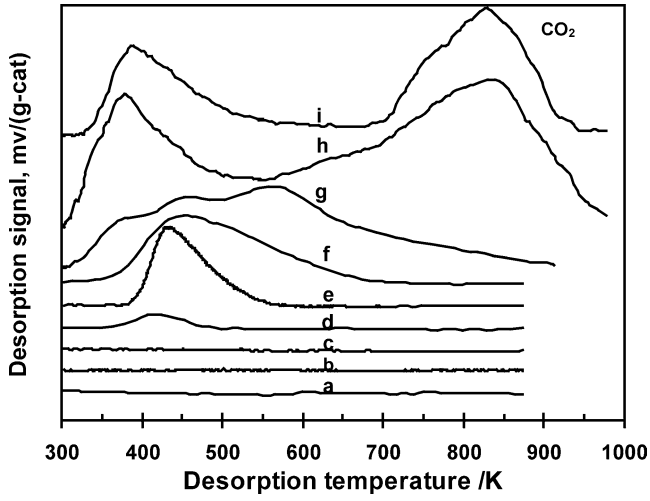

Fig. 4. CO_2-TPD curves of supports (a, AC; b, CNTs; c, ZrO_2-BD; d, TiO_2; e, ZrO_2; f, Al_2O_3; g, MgO; h, K/CNTs; i, K/ZrO_2-BD).

Fig. 4 shows the CO_2-TPD profiles of the supports. One can see that there was almost no CO_2 desorption from AC, CNTs, and ZrO_2-BD. It was suggested before that CNTs is weakly basic [34]; according to our current results, the adopted CNTs after purification are neutral. Small amounts of CO_2 were desorbed from TiO_2 and ZrO_2 and desorption ended up at ca. 550 K, revealing that there are weakly basic sites on these supports. Three peaks centered at 383, 452, and 467 K over MgO and two broad ones at ca. 383 and 839 K over KOH-modified CNTs and ZrO_2-BD samples were observed, showing that there are both weak and strong basic sites on the two KOH-modified support materials. The broad peak at 839 K is possibly related to the decomposition of K_2CO_3, because KOH can react with CO_2 in the course of CO_2 adsorption. Certainly, the results still reflect the presence of strong basic sites on the KOH-modified supports.

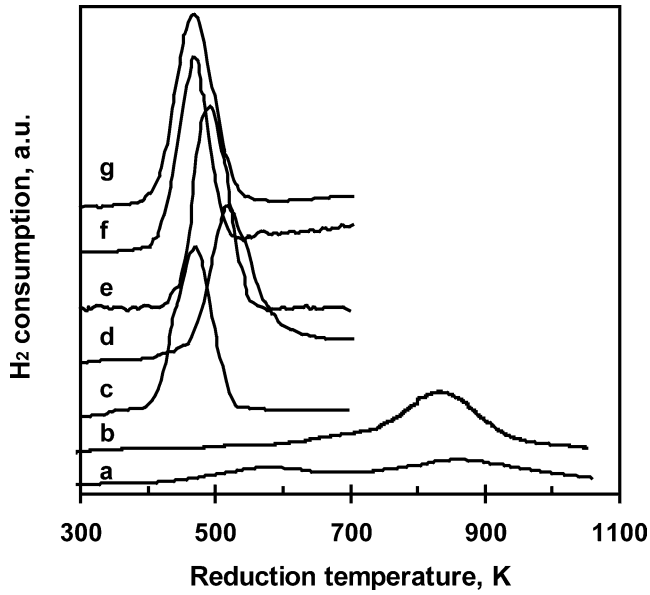

Fig. 5. TPR profiles of CNTs-supported metal catalysts (a, Ni; b, Fe; c, reference RuO_2 without support; d, Ru; e, Pd; f, Rh; g, Pt).

The acid/base natures of MgO, Al_2O_3, ZrO_2, and TiO_2 are similar to those reported in the literature [35,36]. The high surface area ZrO_2-BD support prepared by the reflux-digestion method was found to show higher acidity than the conventional ZrO_2 support. Our previous study showed that during the reflux digestion in basic solution, dissolution of Si^{4+} ions from the glass vessel can result in incorporation of Si^{4+} ions into the sample of ZrO_2-BD [27]. According to the results of colorimetry analysis, the Si content in this ZrO_2-BD sample was 5.0%. The presence of SiO_2 could lead to the elimination of surface basicity on ZrO_2-BD [36–38].

4.4. H_2-TPR

In H_2-TPR studies, one can obtain useful information for catalyst reduction prior to activity evaluation as well as evidence for the interaction between active component and support. Plotted in Figs. 5 and 6 are the TPR profiles of Ru catalysts and CNTs-supported metal catalysts. The calcined precursors of Rh/CNTs, Pd/CNTs, Pt/CNTs, and Ru/CNTs can be completely reduced at a temperature below 673 K, while those of the other two CNT-supported (Ni and Fe) catalysts are more difficult to reduce. The reduction temperatures for the supported Ru catalysts are slightly higher than "pure" RuO_2, implying that there is interaction between support and active component. From Fig. 6, it is apparent that the supports show little effect on the reduction behavior of the supported Ru precursors.

Based on the amounts of H_2 consumption, the reducibility of and oxidation states of the active components in the calcined catalyst precursors can be estimated, respectively. As listed in Table 5, H_2 consumption for all the Ru catalysts is almost identical, independent of support materials, and the reducibility of the active metal components is nearly 100%.

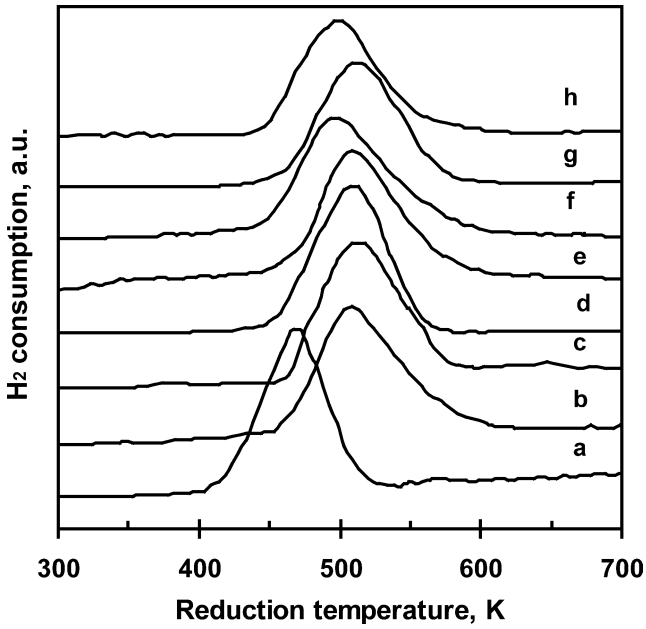

Fig. 6. TPR profiles of Ru catalysts supported on different materials (a, K/CNTs; b, AC; c, Al_2O_3; d, MgO; e, TiO_2; f, ZrO_2-C; g, ZrO_2-BD; h, K/ZrO_2-BD).

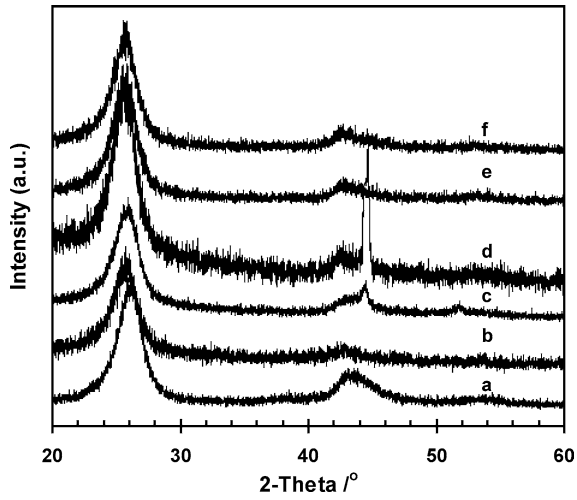

Fig. 7. XRD patterns of CNTs-supported metal catalysts (a, Ru; b, Rh; c, Ni; d, Fe; e, Pt; f, Pd).

The active metals in the calcined precursors are in the form of Fe_2O_3, NiO, RhO_2, RuO_2, PdO_2, and PtO_2, respectively.

4.5. XRD

In the XRD analysis of the reduced CNT-supported catalysts, we observed only the broad diffraction lines (100 and 102) of CNTs (Fig. 7) for the supported noble metal catalysts. The absence of any diffractions attributable to the metals indicates that they are highly dispersed on the CNTs support. But, there are characteristic lines ascribed to Fe ($2\theta = 44.67°$) and Ni ($2\theta = 44.52$, $52.1°$) in the XRD patterns of Fe/CNTs and Ni/CNTs, respectively. With respect to the XRD patterns of the Ru catalysts (Fig. 8), those of Ru/CNTs, RuK/CNTs, and Ru/AC show no diffraction lines related to Ru particles, whereas the other Ru catalysts exhibit characteristic lines of Ru nanocrystals at 44.02, 38.38, and 42.15 (2θ). The results again suggest that CNTs and AC are support materials enabling high Ru dispersion.

Table 5
Properties of catalysts for ammonia decomposition

Sample	H_2-TPR			Chemisorption (μmol/g_{cat})			Activation energy
	H_2 uptake (μmol/g)	Peak temp. (K)	Reducibility (%)	CO	H_2	Dispersion[a] (%)	(E_α, kJ/mol)[b]
CNTs	114	879	–	1.1	0.8	–	–
RuO_2	14,987	465	99.7	–	–	–	–
Ru/CNTs	907	518	97.7	98.2	50.0	21.2	69.2[b], 69.9[c]
Rh/CNTs	912	473	97.2	115.1	50.3	24.5	80.9[b]
Pt/CNTs	914	468	95.0	139.2	61.4	28.9	88.2[b]
Pd/CNTs	925	495	97.2	133.1	62.1	28.0	99.7[b]
Fe/CNTs	703	839	97.2	47.4	31.9	9.8	148.5[b]
Ni/CNTs	476	568,873	97.9	67.9	32.5	14.0	90.3[b]
Ru/AC	914	514	97.4	97.1	52.2	20.7	75.7[c]
Ru/MgO	921	508	96.5	44.2	–	9.3	62.3[c]
Ru/Al_2O_3	917	518	95.5	50.4	–	10.5	64.6[c]
Ru/TiO_2	913	511	97.3	48.5	–	10.3	63.3[c]
Ru/ZrO_2	911	494	95.9	51.4	–	10.8	65.5[c]
Ru/ZrO_2-BD	914	513	95.0	58.4	–	12.1	80.4[c]
RuK/CNTs	864	473	96.6	104.1	–	23.3	56.1[c]
RuK/ZrO_2-BD	850	503	97.0	63.5		14.5	57.2[c]

[a] The dispersion was estimated according to CO-chemisorption data, assuming Ru:CO = 1:1 [18].
[b] The apparent activation energies were obtained from the Arrhenius plots with $GHSV_{NH_3} = 30{,}000$ ml/(h g_{cat}).
[c] The apparent activation energies were obtained from the Arrhenius plots with $GHSV_{NH_3} = 150{,}000$ ml/(h g_{cat}).

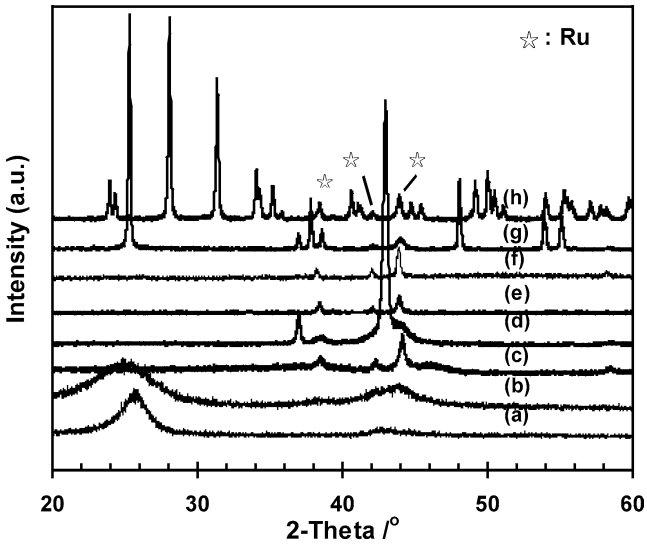

Fig. 8. XRD patterns of Ru catalysts supported on different materials (a, K/CNTs; b, AC; c, Al_2O_3; d, MgO; e, K/ZrO_2-BD; f, ZrO_2-BD; g, TiO_2; h, ZrO_2).

4.6. TEM

In order to investigate the effect of support on the particle size and morphology of the Ru catalysts, we employed the TEM technique. As shown in Fig. 9, the Ru particles on CNTs, K/CNTs, and AC are spherical, and 2–5 nm in size. With tilting operation in the TEM measurement, we detected that some of Ru particles were actually inside the channels of CNTs, while the others on the outer walls. The TEM results of Ru sizes over CNTs and AC are similar to those obtained by HRTEM [25]. On Al_2O_3, MgO, and ZrO_2-BD, the sizes of Ru crystals are in the 3–15 nm range. According to the $d_n = \sum n_i d_i / \sum n_i$ equation depicted in Ref. [39], the average size of Ru particles was estimated based on the random size of 100 particles. We found that the average sizes of Ru nanocrystals on CNTs and AC are around 4.0 nm, smaller than those observed on MgO, ZrO_2-BD, and Al_2O_3. The modification of CNTs with KOH shows only a slight effect on the size of Ru particles.

According to average particle sizes, the dispersions of the Ru catalysts were calculated and are listed in the final column of Table 4. The Ru dispersions on CNTs, K/CNTs, and AC are almost the same, around 25%. Thus, the modification of CNTs with potassium shows little effect on Ru dispersion. The dispersions over Al_2O_3, MgO, and ZrO_2-BD are similar, ca. 12%.

4.7. CO and H_2 chemisorption

First, CO and H_2 chemisorption was conducted over the supports. We observed a small amount of H_2 adsorption (0.1 μmol/g_{CNTs}) over CNTs but zero adsorption over the others. All the supports showed zero capacity of CO adsorption.

The chemisorption capacity of CO on Ru/CNTs, RuK/CNTs, and Ru/AC is rather close, ca. 100 μmol/g_{cat}. The number of exposed metal sites based on CO-chemisorption results agrees well with that indicated by the H_2-chemisorption data. Since the H:metal (e.g., Ni, Ru, Pt) stoichiometry is commonly assumed to be 1, we deduced that the CO:metal stoichiometry is 1:1, consistent with that of Goodman's group [18]. The levels of CO chemisorption over the Ru catalysts supported on the metal oxides are in the 40–60 μmol/g_{cat} range, lower than those over Ru/AC, Ru/CNTs, and RuK/CNTs. We observed no significant difference in chemisorption level between Ru/ZrO_2-BD and RuK/ZrO_2-BD, although that observed over the latter was marginally higher than that over the former. In terms of CO adsorption on the CNT-supported catalysts, both Pt/CNTs and Pd/CNTs adsorb ca. 140 μmol/g_{cat}, while the adsorbed amounts over Rh/CNTs and RuK/CNTs are similar to that over Ru/CNTs. The amounts of CO adsorbed on Ni/CNTs and Fe/CNTs are considerably smaller, 67.9 and 47.4 μmol/g_{cat}, respectively, much lower than those on the noble metal catalysts supported on CNTs.

Based on the chemisorption data and assuming an adsorption of one CO (or H) per metal atom [18], one can estimate the dispersion of the metal catalysts. The dispersions of Pt and Pd are 28–29%, the highest among the present catalysts. The dispersion of Ni is 9.8%, the lowest among the CNTs-based catalysts. The dispersion of Ru over AC, CNTs, and K/CNTs is ca. 21%, significantly better than that over the other supports. Such level of Ru dispersion is higher than that reported by Goodman and co-workers over the 10% Ru/SiO_2 and 10% Ru/Al_2O_3 catalysts [18]. The dispersion figures of Ru/AC and Ru/CNTs are agreeable to the H_2-chemisorption data (118 μmol/g_{cat}) reported by Bradford et al. over Ru/C [16]. As for CO chemisorption, they reported a value of 647 μmol/g_{cat}. They regarded that the large extent of CO adsorption is due to carbonyl formation. We, however, did not find such a large discrepancy between H_2 and CO uptakes over a particular sample. Therefore, we deduce that the formation of carbonyl complexes was not serious in the course of CO adsorption on catalysts of the present study. Moreover, our data indicated that the modification of CNTs and ZrO_2-BD with KOH results in only slight changes in Ru dispersion.

4.8. N_2-TPD

Shown in Fig. 10 are the N_2-TPD patterns of Ru/CNTs, RuK/CNTs, Ru/ZrO_2-BD, and RuK/ZrO_2-BD. Over Ru/CNTs, N_2 desorption begins at 503 K and shows a maximum at 623 K. Over RuK/CNTs, the values are 478 and 607 K, respectively, suggesting that the modification of CNTs with KOH promotes N_2 desorption. We observed similar results in the modification of a reduced Ru/CNTs catalyst with KOH [40]. The N_2-TPD behavior over the KOH-modified samples is similar to those over KRu/C reported by Kowalczyk and co-workers [41]. Compared to Ru/CNTs, Ru/ZrO_2-

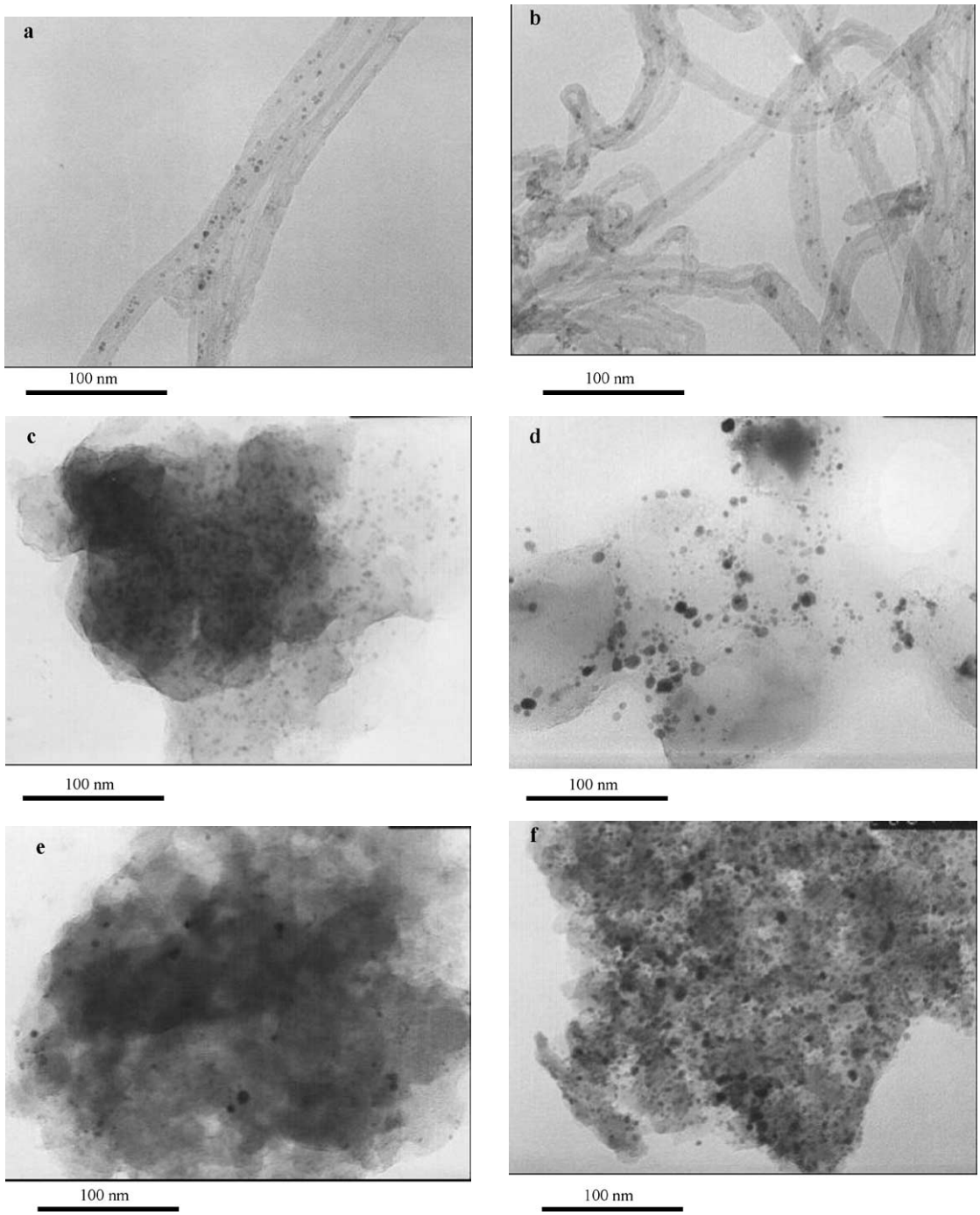

Fig. 9. TEM pictures of Ru catalysts on different supports (a, CNTs; b, K/CNTs; c, AC; d, MgO; e, ZrO_2-BD; f, Al_2O_3).

BD shows a higher temperature of maximum desorption (648 K) but no marked difference in onset temperature. The modification of ZrO_2-BD with KOH results in a similar effect on N_2 desorption.

As for the amount of N_2 desorption, it is 29.2 and 13.1 μmol/g, respectively, over Ru/CNTs and Ru/ZrO_2-BD. The modification of CNTs with KOH led to a slight increase in the amount of desorbed N_2 (31.4 μmol/g), whereas there was a decrease in the case of KOH-modified Ru/CNTs [40]. It is possible that the loading of KOH on Ru/CNTs caused a reduction in the surface area of Ru. The modification of ZrO_2-BD with KOH resulted in ca. 9% increase in the N_2 desorption.

5. Discussion

The results of Ru dispersion based on the chemisorption data are in good agreement with those of TEM and XRD; Ru dispersion is good on CNTs and AC supports. One explana-

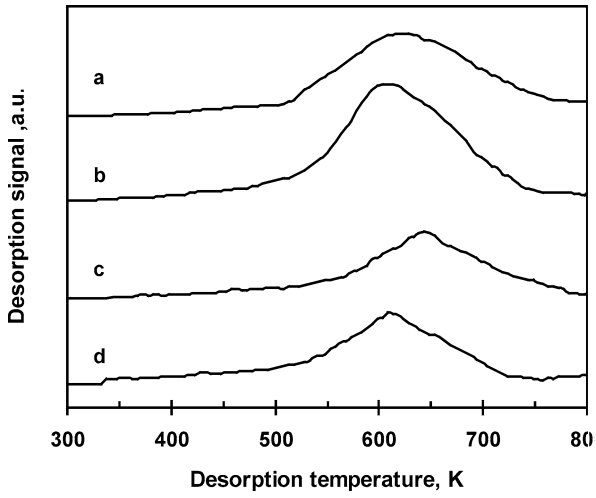

Fig. 10. N_2-TPD curves over three Ru catalysts (a, Ru/CNTs; b, RuK/CNTs; c, Ru/ZrO_2-BD; d, RuK/ZrO_2-BD).

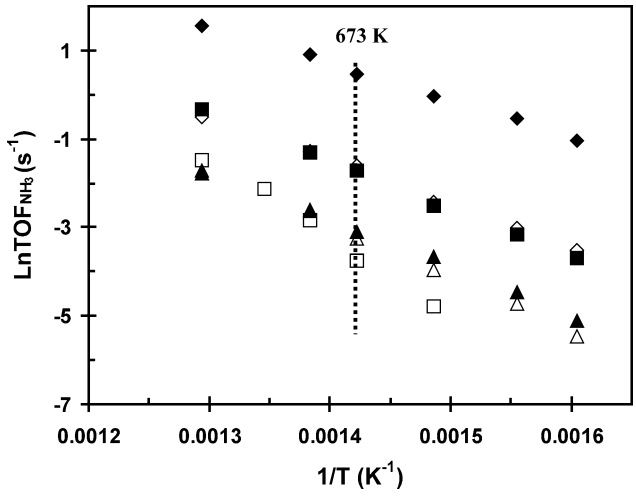

Fig. 11. Arrhenius plots of CNT-supported metal catalysts (◆, Ru; ■, Ni; ◇, Rh; △, Pd; □, Fe; ▲, Pt).

tion is that AC and CNTs are high in surface area, and being nanosize, the CNTs material restricts the growth of Ru particles. It is known that there are various functional groups (e.g., –COOH, –OH) on CNTs and AC [42] that cause a negative effect on the electronic structure of metal catalyst in NH_3 decomposition and synthesis. However, it is possible that such groups are responsible for the anchoring of the metal on the carbon materials. In addition, because of the strong oleophylic ability of CNTs and AC, the use of acetone as solvent for $RuCl_3$ is beneficial for the anchoring of Ru precursor. Previously, we found that the use of water as solvent would result in Ru particles of larger sizes on CNTs [40]. The poor dispersion of Ru on the metal oxide supports is possibly related to a different kind of interaction between the support oxides and Ru precursor during the impregnation and drying processes.

The results so far show that Ru/CNTs and RuK/CNTs are promising catalysts for on-site generation of H_2 from NH_3. We ascribed the high activity to the high dispersion of Ru, and to the high graphitization and purity of CNTs [25]. Generally speaking, the catalytic performance of a catalyst is dependent on (i) acidity and/or basicity of support, (ii) interaction of active sites with reactants and/or products, (iii) surface area and structure of catalyst and/or support, and (iv) resistance to sintering. Despite that the surface area of Ru/CNTs is much lower than that of Ru/AC, the catalytic activity of the former is much higher than that of the latter. Also, Ru/ZrO_2 is catalytically more active than Ru/ZrO_2-BD, though the surface area of the latter (223 m^2/g) is 11 times larger than that of the former (19 m^2/g). Therefore, it seems that surface area is not a determining factor for good performance of the supported Ru catalysts. The results of the XRF study showed that the Cl ions in the catalysts of unmodified supports are small and similar in concentration. Another study on the stability of Ru/CNTs catalyst disclosed that over a TOS of ca. 30 h, a slight (< 5%) increase in ammonia conversion (from 43.71 to 45.53%) was observed [40]. Similar results were observed over the other catalysts of unmodified supports. Thus, despite that residual chlorine has been considered as a strong inhibitor for ammonia decomposition/synthesis catalysts [10,31–33], its negative effect on the activity of the present catalysts of unmodified supports can be considered as negligible.

5.1. Comparison of active component

As a standard parameter for catalytic performance, TOF is calculated by normalizing the observed reaction rates (molar conversion, $NH_3/(s\,g_{cat})$) to the number of exposed Ru sites (atoms per gram). The Arrhenius plots of the CNT-supported catalysts are shown in Fig. 11. Obviously, at a reaction temperature of 673 K, the TOFs on the CNT-supported metal catalysts can be arranged in the order of Ru > Rh ≅ Ni > Pt ≅ Pd > Fe. The ranking is nearly similar to that of NH_3 conversions over the metal catalysts. Therefore, supported Ru is the most active catalyst for NH_3 decomposition, similar to the reported results in NH_3 synthesis [10] and decomposition [13,18]. The TOF in the present Ru catalyst is slightly lower than that reported by Goodman et al., because the Ru particles in their work are much bigger than the Ru particles on CNTs [18]. In ammonia synthesis, it has been reported that the larger the particle size of Ru on carbon support, the more active the catalyst in terms of TOF value [43]. A similar trend was observed over the Ru catalysts of different supports in the present study. Till now, there has been no clear explanation for such an experimental observation. We cannot compare the present TOF results with those of the others in the literature due to difference in reaction conditions.

The apparent activation energies (E_α) based on the Arrhenius plots are listed in Table 5. The E_α values for Ru/CNTs, obtained at different hourly space velocities of ammonia [i.e., 69.2 kJ/mol at $GHSV_{NH_3}$ = 30,000 $ml/(h\,g_{cat})$; 69.9 kJ/mol at $GHSV_{NH_3}$ = 150,000 $ml/(h\,g_{cat})$]

are reasonably close. This fact excludes any possible involvement of mass transfer and equilibrium limitations that could affect the E_α values. The E_α of Ru/CNTs is the lowest among the metal catalysts; it is interesting to note that the value is lower than those reported for Ru/SiO_2 (19.0 kcal/mol, i.e., 79.6 kJ/mol) and Ru/Al_2O_3 (19.5 kcal/mol, i.e., 81.5 kJ/mol) [18]. The apparent activation energies of the Rh, Ni, and Pt catalysts are within the 80.9 to 90.3 kJ/mol range, while those of the Pd and Fe catalysts are 99.7 and 148.5 kJ/mol, respectively. Papapolymerou and Bontozoglou [13] found that the apparent activation energies for the decomposition reaction over polycrystalline Pt and Rh wires are both 21 kcal/mol (i.e., 87.8 kJ/mol), while over Pd wires, it is 26.2 kcal/mol (i.e., 109.5 kJ/mol). The E_α of the Ni/CNTs catalyst is similar to those of Ni/SiO_2 and $Ni/SiO_2/Al_2O_3$ [18]. The E_α of KRu/C and KFe/C catalysts reported by Kowalczyk and co-workers [22] are 139 and 166 kJ/mol, respectively, much higher than those of the present CNT-supported catalysts. Previously, Bardford et al. [16] showed that in NH_3 synthesis and decomposition, reaction conditions can exert great influences on the E_α of Ru catalysts.

5.2. Effect of the basicity of support

Illustrated in Fig. 12 is the effect of supports on the TOF of the Ru catalysts. Unlike the CNT-supported ones, the order of TOF over the Ru catalysts is support dependent and is different from the order of NH_3 conversions. Despite that the NH_3 conversion over Ru/CNTs is higher than that over Ru/MgO, the TOF of the former is lower than that of the latter. The TOF of RuK/CNTs is higher than that of Ru/MgO. Among all the catalysts, the TOF over Ru/AC is the second lowest, only higher than that over ZrO_2-BD.

The apparent activation energies (E_α) of Ru catalysts on different support materials are also listed in Table 5. The E_α values of the Ru catalysts on the metal oxide supports except that of ZrO_2-BD are in the range of 62–66 kJ/mol, lower than those over the CNTs- and AC-supported Ru catalysts. The E_α is 69.9 kJ/mol for the Ru/CNTs and 80.4 kJ/mol for Ru/ZrO_2-BD. The modification with KOH results in a marked decrease in E_α of the Ru/CNTs and Ru/ZrO_2-BD catalysts. The E_α is 56.1 kJ/mol for RuK/CNTs and 57.2 kJ/mol for RuK/ZrO_2-BD.

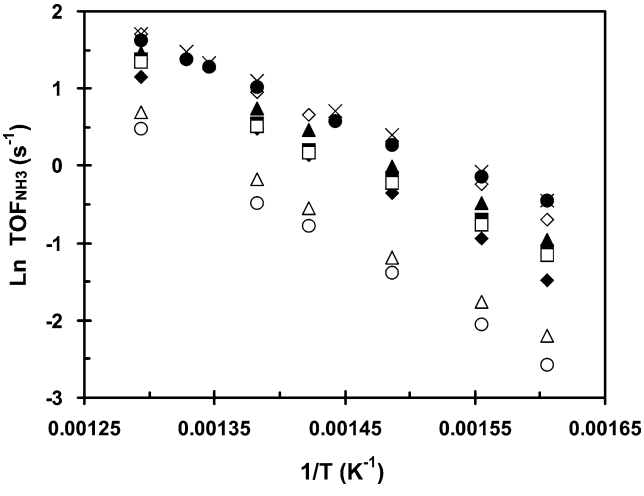

Fig. 12. Arrhenius plots of Ru catalysts on different supports (◆, CNTs; ◇, MgO; ▲, TiO_2; △, AC; ■, Al_2O_3; □, ZrO_2; ○, ZrO_2-BD; ●, K/ZrO_2-BD; ×, K/CNTs).

According to the TOF and E_α data, the order of catalyst activity can be ranked according to the order of increasing basicity of the support materials. The TOF over the Ru catalyst using basic MgO as support is the highest among the unmodified catalysts. On the other hand, the NH_3 conversion and TOF over the Ru catalyst using acidic ZrO_2-BD as support is the lowest among the present Ru catalysts. The increase in basicity of neutral CNTs and acidic ZrO_2-BD due to KOH modification results in a marked increase in both NH_3 conversion and TOF. We deduce that a support of high acidity is unsuitable for NH_3 decomposition, whereas a support of high basicity is necessary for high catalytic efficiency.

It is noted that after hydrogen reduction at high temperature, residual chlorine in the Ru catalysts of unmodified supports is almost completely removed. The stability of activity also suggests that the negative effect of residual chlorine on the catalysts is negligible. As for the RuK/CNTs and RuK/ZrO_2-BD catalysts, the Cl/Ru molar ratios are ca. 4–20 times higher than that of the unmodified supports. Due to the partial conversion of KOH to KCl, the amount of KOH available on the modified supports was reduced after the loading of $RuCl_3$. We believe that most of the potassium still exists as KOH. After refluxing the reduced RuK/CNTs and RuK/ZrO_2-BD samples in deionized water (solid/liquid ratio 1/5) at 370 K for 4 h, we found that the water turned basic, confirming that the two catalysts are still strongly basic. Hence, despite the negative effect of residual Cl, the activities of RuK/CNTs and RuK/ZrO_2-BD are still higher than that of the corresponding Ru/CNTs and Ru/ZrO_2.

In NH_3 synthesis, Aika and co-workers [32] observed that the activities of supported Ru catalysts could be arranged according to support electronegativity; the higher the electronegativity, the lower the activity. Furthermore, the extent of such support effect shows an inverse relationship with the electronegativity of the compounds adopted for Ru/MgO modification. The activities of Ru catalysts can be ranged in the order of the basicity of supports or promoter/supports: Al_2O_3 < MgO < Cs/Al_2O_3 (Cs/Ru = 8 mol/mol) < Cs/MgO (Cs/Ru = 0.1 mol/mol) < Cs/MgO (Cs/Ru = 1.0 mol/mol). Using FTIR to study the effect of promoter, Aika et al. found that with the increase of support basicity, the vibration frequency of adsorbed N_2 shifts to a lower wavenumber. They considered that activity enhancement is due to electron transfer from the promoter to Ru [44]. It should be noted that for both ammonia synthesis and decomposition, the use of acidic support for metal catalysts is rare. One reason for that is an acidic support means strong NH_3

adsorption; the other reason disclosed by the present study is that being an electron-withdrawing material, an acidic support exerts a negative effect on NH_3 decomposition, an aspect to be discussed in the next subsection.

Additionally, we observed that the TOFs of the Ru catalysts show a declining tendency when the size of the Ru particles becomes smaller or the Ru dispersion level becomes higher.

5.3. Reaction kinetics of NH_3 decomposition

The N_2-TPD results (Fig. 10) and TOF data (Fig. 12) disclose that the lower the temperature for N_2 desorption, the larger the TOF over the Ru catalysts, suggesting that the desorption of N_2 is the rate-determining step in NH_3 decomposition. Moreover, a higher temperature of N_2 desorption means higher apparent activation energy over the Ru catalysts. With respect to the CNT-supported catalysts, we found that the higher the TOF, the lower the apparent activation energy. Although we are unable to disclose the chemical nature of the key reaction intermediate on these catalyst, it is still highly possible that desorption of N_2 is the slowest step in NH_3 decomposition over the catalysts used in the present study.

Boudart et al. [45] proposed that over W and Mo, (i) the breaking of N–H bonds, (ii) the combination of two N atoms, and (iii) the desorption of N_2 are slow irreversible steps during NH_3 decomposition. Despite certain subtle differences, the results of experiments conducted on Pt and Ru by Loffler et al. [46], Tsai et al. [47], and Bradford et al. [16] advocate such a proposition. Apparently, the acid-base nature of the supports exerts certain effects on N_2 desorption and hence on the TOF over the Ru catalysts.

It was reported that electron transfer from support to Ru facilitates the recombinative desorption of surface N atoms [16]. We observed that in KOH modification of Ru catalysts supported on conductive CNTs and nonconductive MgO, the effect of modification was more prominent over the former case [25]. This is because electron transfer from promoter to Ru is more feasible in the case of a conductive support. Certainly, the promotional effect is also dependent on the adopted active component. In another set of experiments, we observed that KOH modification can also result in activity enhancement of a Ni/ZrO_2 catalysts for NH_3 decomposition, although the degree of enhancement is much lower than that observed over the Ru-based catalyst.

6. Conclusion

The metallic Ru catalyst is highly active for the generation of CO_x-free H_2 from ammonia, and CNTs are an excellent support material for the catalyst. The dispersion of Ru on CNTs is the highest among all the support materials examined in this study. The modification of CNTs and ZrO_2-BD with KOH results in a significant enhancement in the catalytic activity of supported Ru catalyst. A support of basic nature is required for high catalytic efficiency, and an increase in the support basicity leads to TOF enhancement of the Ru catalysts. The apparent activation energies of the reaction over Ru catalysts are dependent on the property of materials adopted as the catalyst support. The desorption of N_2 appears to be the rate-determining step in the catalytic NH_3 decomposition reaction. The results also implied that, if a support having both strong baisicity and good electronic conductivity is used as the support for Ru catalyst, it is possible to develop a more efficient catalyst for the generation of CO_x-free hydrogen from ammonia.

Acknowledgments

This work was supported by RGC, HKSAR (Grant HKBU 2037/00P) at HKBU, and NSF, China (Grant 20125310), at Tsinghua University. B.Q.X. thanks the Croucher Foundation for a visitorship to HKBU.

References

[1] A.S. Chellappa, C.M. Fischer, W.J. Thomson, Appl. Catal. A 227 (2002) 231.
[2] J.R. Rostrup-Nielsen, in: J.R. Anderson, M. Boudart (Eds.), Catalytic Steam Reforming, Science and Engineering, vol. 5, Springer, Berlin, 1984.
[3] T.V. Choudhary, D.W. Goodman, Catal. Lett. 59 (1999) 93.
[4] T.V. Choudhary, D.W. Goodman, J. Catal. 192 (2002) 316.
[5] V.R. Choudhary, B.S. Uphade, A.S. Mamman, J. Catal. 172 (28) (1997) 1.
[6] J.N. Armor, Appl. Catal. A 176 (1999) 159.
[7] R. Metkemeijer, P. Achard, Int. J. Hydrogen Energy 19 (1994) 535.
[8] R. Metkemeijer, P. Achard, J. Power Sources 49 (1994) 271.
[9] W. Arabczyk, J. Zamlynny, Catal. Lett. 60 (1999) 167.
[10] W. Raróg, D. Smigiel, Z. Kowalczyk, S. Jodzis, J. Zielinski, J. Catal. 218 (2003) 465.
[11] J. Hepola, P. Simell, Appl. Catal. B 14 (1997) 287.
[12] P.A. Simell, J.O. Hepola, A.O. Krause, Fuel 76 (1997) 1117.
[13] G. Papapolymerou, V. Bontozoglou, J. Mol. Catal. A: Chem. 120 (1997) 165.
[14] J.-G. Choi, J. Catal. 182 (1999) 104.
[15] K. Hashimoto, N. Toukai, J. Mol. Catal. A: Chem. 161 (2000) 171.
[16] M.C.J. Bradford, P.E. Fanning, M.A. Vannice, J. Catal. 172 (1997) 479.
[17] H. Dietrich, K. Jacobi, G. Ert, Surf. Sci. 352–354 (1996) 138.
[18] T.V. Choudhary, C. Svadinaragana, D.W. Goodman, Catal. Lett. 72 (2001) 197.
[19] D.A. Goetsch, S.J. Schmit, WO patent 0 187 (2001) 770.
[20] K. Kordesch, V. Hacker, R. Fankhauset, G. Faleschini, WO patent 0 208 (2002) 117.
[21] M.E.E. Abashar, Y.S. Al-Sughair, I.S. Al-Mutaz, Appl. Catal. A 236 (2002) 35.
[22] A. Jedynak, Z. Kowalczyk, D. Smigiel, W. Rarog, J. Zielinski, Appl. Catal. A 237 (2002) 223.
[23] M.E.E. Abashar, Chem. Eng. Proc. 41 (2002) 403.
[24] C.W. Robert, in: CRC Handbook of Chemistry and Physics, CRC Press, FL, 1983, p. D-77.
[25] S.F. Yin, B.Q. Xu, C.F. Ng, C.T. Au, Appl. Catal. B, in press.

[26] Y. Wang, F. Wei, G.H. Luo, H. Yu, G.S. Gu, Chem. Phys. Lett. 364 (2002) 568.
[27] S.F. Yin, B.Q. Xu, Chem Phys Chem. 3 (2003) 277.
[28] S.F. Yin, B.Q. Xu, Chin. J. Catal. 23 (2002) 507.
[29] R.B. Strait, Nitrogen Methanol 238 (1999) 37.
[30] P.B. Weisz, Chem. Eng. Prog. Ser. 55 (1959) 29.
[31] O. Hinrichsen, Catal. Today 53 (1999) 177.
[32] S. Murata, K.I. Aika, J. Catal. 136 (1992) 110; J. Catal. 136 (1992) 118; J. Catal. 136 (1992) 126; J. Catal. 173 (1998) 535.
[33] Z.H. Zhong, K.I. Aika, Inorg. Chim. Acta 280 (1998) 183.
[34] M.W. Wang, F.Y. Li, N.C. Peng, New Carbon Mater. 17 (2002) 75.
[35] K. Tanable, Mater. Chem. Phys. 13 (1985) 347.
[36] K. Tanabe, M. Misono, Y. Ono, H. Hattori, New Solid Acids and Bases, Kodansha–Elsevier, 1989.
[37] S. Soled, G.B. Mcvicker, Catal. Today 14 (1992) 189.
[38] M. Niwa, N. Katada, Y. Murakami, J. Catal. 134 (1992) 340.
[39] Y.G. Yin, in: Experimental Methods in Heterogeneous Catalyst, Chemical Industry Press, Beijing, 1988, p. 197.
[40] S.F. Yin, B.Q. Xu, W.X. Zhu, C.F. Ng, C.T. Au, submitted for publication.
[41] W. Rarog, Z. Kowalczyk, J. Sentek, D. Skladanowski, D. Szmigiel, J. Zielinski, Appl. Catal. A 208 (2001) 213.
[42] J. Kastner, T. Pichler, H. Kuzmany, Chem. Phys. Lett. 221 (1994) 53.
[43] C.H. Liang, Z.B. Wei, Q. Xin, C. Li, Appl. Catal. A 208 (2001) 193.
[44] K. Aika, J. Kubota, Y. Kadowaki, Y. Niwa, Y.Y. Izumi, Appl. Surf. Sci. 121/122 (1997) 488.
[45] M. Boudart, G. Djega-Mariadassou, in: Kinetics of Heterogeneous Catalytic Reactions, Princetone Univ. Press, Princeton, NJ, 1984, p. 98.
[46] D.G. Löffler, L.D. Schmidt, J. Catal. 41 (1976) 40.
[47] W. Tsai, W.H. Weinberg, J. Phys. Chem. 91 (1987) 5307.